INTERNATIONAL JOURNAL FOR NUMERICAL METHODS IN FLUIDS
Int. J. Numer. Meth. Fluids 2002; **38**:647–675 (DOI: 10.1002/fld.236)

Iterative explicit simulation of 1D surges and dam-break flows

Chih-Tsung Hsu*,† and Keh-Chia Yeh

Department of Civil Engineering, National Chiao Tung University, Hsinchu, 30050 Taiwan, Republic of China

SUMMARY

The one-dimensional Saint Venant equations for shallow-water flows are used to simulate the flood wave resulting from the sudden opening (or closure) of a gate or collapse of a dam. An iterative explicit characteristics-based finite-difference method, based on the explicit finite analytic method, is proposed to discretize the dynamic equation, and the conservative control volume method is used for the discretization of the continuity equation. Surge and dam-break flows in a horizontal, rectangular and frictionless channel were first considered, under such conditions the analytic solutions exist. For the surge simulation, numerical results of the proposed scheme are nearly identical to those obtained from the Preissmann scheme. For the dam-break simulations addressing three ratios of tailwater depth to water depth in the reservoir, the proposed scheme, as compared with the analytic solutions, yields better results than those obtained by the MacCormack scheme, the Gabutti scheme, and Jha *et al*.'s flux splitting scheme (*J. Hydraul. Res*. 1996; **34**(5):605–621). As the depth ratio approaches zero, the accuracy of the proposed scheme is still satisfactory, even with the dry-bed condition. Investigations then were made for more realistic dam-break flow waves propogating in a sloped and frictional channel. Lacking analytic solutions, the simulating results from the proposed scheme as well as those from Chen's scheme (*J. Hydraul. Div.* 1980; **106**(HY4):535–556) were compared with the laboratory data collected in 1960–1961 at the United States Army Engineer Waterways Experiments Station (WES). An assumed initial flow was required for the computer-simulated condition in Chen's model. However, this is not the case in the proposed model, i.e., a real dry-bed condition was set as the initial condition in the downstream channel of the dam. The consistency between the two simulated results is obvious compared with the experimental data. Copyright © 2002 John Wiley & Sons, Ltd.

KEY WORDS: iterative explicit scheme; surge; dam-break wave; explicit finite analytic method; staggered-grid

1. INTRODUCTION

The task of estimating the movement of a surge (or shock) or a dam-break wave, resulting from the sudden upstream opening (or the sudden downstream closure) of a sluice gate for emergencies or dam failures, has occupied the attention of researchers as well as practicing engineers for several decades. The determination of the surge height at different locations along the channel provides important information for the design of the bank height. The

*Correspondence to: Chih-Tsung Hsu, Department of Civil Engineering, National Chiao Tung University, 1001 Ta Hsueh Road, Hsinchu, Taiwan 30050.
†E-mail: u8316529@cc.nctu.edu.tw

Received January 2000
Revised March 2001

dreadful disaster due to the dam-break flood wave reminds the decision- makers to pay more attention to the dam-safety problem.

The rapid varied flows in open channels, with steep fronts resulting from surges or dam-break waves, are often simulated as one-dimensional (1D) flows. Such flows can be described by the Saint Venant equations (shallow-water equations), which are a set of non-linear hyperbolic partial differential equations. However, the analytic solutions of these equations are not available, except for certain special simplified conditions. Therefore, consistent efforts have been made to develop numerical schemes to solve the equations. There are three basic approaches to compute the equations of flows with steep fronts: the shock fitting, pseudo-viscosity, and 'through' (shock capturing) methods [1]. The shock fitting method requires internal boundary conditions to determine the position and the associated flow characteristics of the shock, yielding a complicated solution algorithm. The pseudo-viscosity method, which is a common practice adopted in the non-dissipative finite-difference schemes, operates by adding an artificial diffusion term to suppress the oscillation near the front. The 'through' method is most often used in practice because it solves the Saint Venant equations directly without any particular arrangements of the algorithm. The proposed scheme in this paper belongs to the 'through' method.

Many shock capturing schemes are available as described in the literature below. To check their applicability to the real conditions of wave propagations, the simulated results were usually compared to the analytical solutions of the shocks propagating in a 1D horizontal, frictionless channel first, then to the experimental data in a sloped, frictional channel. The numerical schemes using the finite-difference method include the Preissmann four-point scheme [2], Holly–Preissmann two-point together with the reach-back characteristics scheme [3], MacCormack scheme [4–7], Lambda scheme [7], Gabutti scheme [7], Beam-Warming scheme and its modifications [8–10], flux difference splitting scheme [11–14], Godunov-type upwind scheme with a Riemann solver [13, 15–19], modified Godunov scheme [20], total variation diminishing (TVD) scheme [21–23], and semi-Lagrangian scheme [24]. Additionally, the numerical schemes using the finite-element method include the Eulerian–Lagrangian linked Galerkin scheme [25], the dissipative Galerkin scheme [26–28], Petrov–Galerkin scheme [18, 29], Taylor–Galerkin scheme [30], and Addcollocation scheme [31]. Additionally, the explicit scheme by Cheng-lung Chen mentioned above used the characteristics method.

The numerical schemes used for solving the dam-break problem face severe challenges when they are applied to cases characterized by large upstream water depths (h_u) in the reservoirs and small downstream water depths (h_d) in the channels. A mixed-flow regime (i.e., supercritical and subcritical flows co-exist) occurs for flows in the horizontal, frictionless channels when the value of h_d/h_u is smaller than 0.138 [32]. This flow regime is difficult to be handled by the numerical schemes. Furthermore, the height, shape, and celerity of the simulated front under such a condition may significantly deviate from the exact solution [11]. Under the extreme condition of dry bed ($h_d = 0$), few of the above mentioned numerical schemes [15, 33] can work because it is not easy to deal with the moving boundary condition of zero water depth. To cope with this difficulty, a commonly used technique in numerical computation is to assume that a minimum water depth or discharge exists on the dry bed of the channel. As pointed out by Zhang *et al.* [34], the accumulated error due to this assumption as the computation proceeds might eventually distort the solutions and hence render the numerical solution near the wave front doubtful. Therefore, Zhang *et al.* [34] proposed an implicit staggered-grid scheme, analogous to the SIMPLER method [35], to analyze the dam-break

problems on dry beds. Bellos and Sakkas [36] employed the explicit MacCormack scheme with an expedient treatment to determine the computational grid at the boundary, wet or dry, to solve the same problem. Moreover, Di Monaco and Molinaro [37] developed a Lagrangian model for simulating the dam-break waves on dry beds using the finite-element method.

The purpose of this paper is to propose an iterative explicit characteristics-based finite-difference scheme suitable for the computation of surges and dam-break waves propagating both in rectangular, horizontal, and frictionless channels and in sloped, and frictional channels. The proposed scheme is a modification of the explicit finite analytic (FA) method, which was first employed by Dai [38] for the computation of 2D and 3D cavity flows. In his scheme, based on the flow conditions of the previous time step, the convective transport equation is solved with a local analytic solution and the viscous diffusion and source terms are approximated by the finite differences. In this paper, the time dependent variables, including the linearized characteristic curve, are updated by the newly calculated flow conditions in the process of iterative computation during a time step. The superiorities of accuracy and simplification of the proposed scheme to other numerical schemes for the dam-break problem can be seen under various cases as well as the most critical dry-bed case.

2. GOVERNING EQUATIONS

The 1D unsteady free-surface flow in a wide rectangular channel without lateral flow can be described by the well-known Saint Venant equations, those based on the conservation of mass and momentum of the conservative form:

$$\frac{\partial h}{\partial t} + \frac{\partial q}{\partial x} = 0 \tag{1}$$

$$\frac{\partial q}{\partial t} + \frac{\partial}{\partial x}\left(uq + \frac{1}{2}gh^2\right) = gh(S_0 - S_f) \tag{2}$$

where h is flow depth; u is flow velocity; q is volumetric flow rate per unit width; t is time; x is distance along the channel; g is gravitational acceleration; S_0 is bed slope; and S_f is frictional slope. The key assumptions in the governing equations are the hydrostatic pressure distribution and small bed slope. The applicability of the Saint Venant equations to surges and dam-break flows with steep fronts, i.e., those with large surface curvatures, has been examined by Basco [39]. He concluded that the Saint Venant equations are valid if the wave period of the input hydrograph is greater than about 100 seconds. Fortunately, most flood waves resulting from dam breaks of practical interest have periods much larger than this value.

For open channel flows with steep fronts, the convective terms in Equation (2) dominate. Thus, Equation (2) can be written in the total derivative form based on the concept of the characteristics method

$$\frac{Dq}{Dt} = -gh\frac{\partial h}{\partial x} - q\frac{\partial u}{\partial x} + gh(S_o - S_f) \tag{3}$$

along

$$\frac{dx}{dt} = u \tag{4}$$

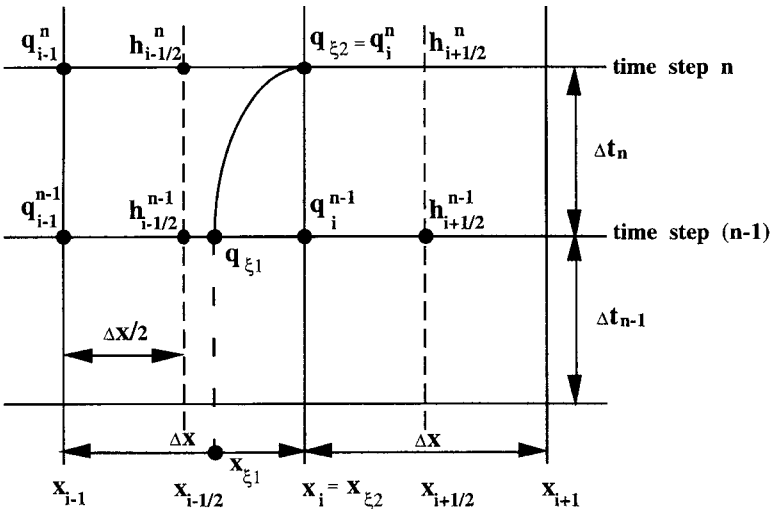

Figure 1. Sketch of characteristic curve and staggered-grid system.

where Dq/Dt is the total derivative of q along the characteristic curve described by Equation (4). The explicit FA method [38] assumes that the variation of u in Equation (4) and the source terms on the right-hand side of Equation (3) are relatively small in a given time increment Δt_n (Figure 1), and can be simplified as known constants. Consequently, Equation (3) reduces to a linear hyperbolic partial differential equation and has the analytic solution ($q_{\xi 2}$) at time step n if the initial condition ($q_{\xi 1}$) at the previous time step ($n-1$) is specified. In such a case, the characteristic is a straight line. In this paper, however, the time dependence of u and the source terms are further considered. Hence, the integration of Equations (3) and (4) can be solved numerically and can be expressed as

$$q_{\xi 2} - q_{\xi 1} = \int_{t_{\xi 1}}^{t_{\xi 2}} -\left(gh\frac{\partial h}{\partial x} + q\frac{\partial u}{\partial x}\right) + gh(S_o - S_f)\,\mathrm{d}t \tag{5}$$

$$x_{\xi 2} - x_{\xi 1} = \int_{t_{\xi 1}}^{t_{\xi 2}} u\,\mathrm{d}t \tag{6}$$

where the subscripts $\xi 1$ and $\xi 2$ denote the foot and the head of the characteristic, respectively (see Figure 1).

3. ITERATIVE EXPLICIT SCHEME

3.1. Discretization

To avoid the so-called 'checkerboard' phenomenon of the computational results, a staggered-grid system (Figure 1) is used in the proposed iterative explicit scheme, which is also adopted

in Dai's approach [38]. Discretization of Equations (1) and (5) results in

$$h_{i+1/2}^{n'} = h_{i+1/2}^{n-1} - \left[\theta\frac{\Delta t_n}{\Delta x}(q_{i+1}^{n'} - q_i^{n'}) + (1-\theta)\frac{\Delta t_n}{\Delta x}(q_{i+1}^{n-1} - q_i^{n-1})\right] \tag{7}$$

$$\begin{aligned} q_i^{n'} = q_{\xi 1} - \{&\theta[gh_i^{n'}(\Delta\nabla h^{n'}) + q_i^{n'}(\Delta\nabla u^{n'}) - gh_i^{n'}(S_o - S_f)_i^{n'}] \\ &+ (1-\theta)[gh_{\xi 1}(\Delta\nabla h^{n-1}) + q_{\xi 1}(\Delta\nabla u^{n-1}) - gh_{\xi 1}(S_o - S_f)_{\xi 1}]\}\Delta t_n \end{aligned} \tag{8}$$

where

$$S_f = \frac{N^2 u^2}{R^{4/3}}$$

and N is Manning coefficient; R is hydraulic radius; $\phi^{n'}(\phi = q, h \text{ or } u)$ denotes the newly updated value of the variables during the iteration at the present time step n; θ is the weighting factor in time; Δt_n is the time interval, which is determined by the Courant condition for ensuring the stability of the explicit scheme; Δx is the subreach length; and $\phi_{\xi 1}$ is approximated by the linear interpolation of ϕ_{i-1}^{n-1} and ϕ_i^{n-1}

$$\phi_{\xi 1} = \phi_i^{n-1}\frac{x_{\xi 1} - x_{i-1}}{\Delta x} + \phi_{i-1}^{n-1}\frac{x_i - x_{\xi 1}}{\Delta x} \tag{9}$$

where $x_{\xi 1}$ is obtained from Equation (6) with the following approximation:

$$x_{\xi 1} = x_i - u_{i-1/2}^{n'}\Delta t_n \tag{10}$$

Note that the source terms $\partial h/\partial x$ and $\partial u/\partial x$ in Equation (8) are discretized by the difference scheme, which is represented by the symbol $\Delta\nabla$. In the subcritical-flow regime, a central difference scheme is adopted to consider the physical phenomenon that the disturbance waves travel both downstream and upstream. On the other hand, due to the unique direction of the traveling disturbance waves in the supercritical-flow regime, the above two terms are discretized by the upwind scheme, i.e., forward or backward difference scheme according to the direction of flow velocity.

3.2. *Boundary conditions*

Unique discrete solutions at each cross-section of a channel at each time step, based on Equations (7) and (8), exist when the initial and boundary conditions are properly specified. The initial conditions include the values of q and h at $t = 0$. As for the boundary conditions, it should be recalled that the only general technique available for dealing with the boundary conditions is the method of characteristics [3, 5, 40] based on the equations:

$$\left[\frac{\partial q}{\partial t} + c^-\frac{\partial q}{\partial x}\right] + a^-\left[\frac{\partial h}{\partial t} + c^-\frac{\partial h}{\partial x}\right] = gh(S_o - S_f) \tag{11}$$

$$\left[\frac{\partial q}{\partial t} + c^+\frac{\partial q}{\partial x}\right] + a^+\left[\frac{\partial h}{\partial t} + c^+\frac{\partial h}{\partial x}\right] = gh(S_o - S_f) \tag{12}$$

where

$$c^- = u - \sqrt{gh}, \quad a^- = -u - \sqrt{gh};$$
$$c^+ = u + \sqrt{gh}, \quad a^+ = -u + \sqrt{gh}.$$

When the flow is supercritical, two boundary conditions related to $q(t)$ and $h(t)$, or $q(h)$ should be provided at the upstream boundary of the channel and Equations (11) and (12) are used to determine the flow conditions at the downstream boundary. When the flow is subcritical, one boundary condition should be provided at the upstream boundary and Equation (11) is used to determine the other flow condition; same to the downstream boundary but Equation (12) is used. The method has been applied to solve the seaward boundary in predicting the flow characteristics on rough slopes for specified, normally incident wave trains by Kobayashi *et al.* [40], and the external and internal boundaries for rapidly varying open channel flows by Garcia-Navarro and Saviron [5].

However, under subcritical flow condition, it is usually difficult to specify the downstream boundary condition, especially for unsteady flow, except that experimental or field measured data can be obtained. The assumption of uniform flow condition or the method of extrapolation from the neighbouring points in the computational domain is taken to provide the boundary condition in some numerical methods. In this paper, as will be described below, an approach based on the characteristic concept is introduced to approximate the flow variables, both q and h, at downstream boundary.

In order to determine the two variables q and h at the downstream boundary, one more equation is needed to be solved simultaneously with Equation (12). The continuity equation is rewritten in the following form:

$$\frac{\partial h}{\partial t} + c\frac{\partial h}{\partial x} = -h\frac{\partial u}{\partial x} \quad (c = u) \tag{13}$$

Figure 2 shows the grid points and the two corresponding characteristic lines of Equation (12) (labeled c^+) and Equation (13) (labeled c) near the downstream end are shown. The values of variables at points L and R have to be determined to make the solution progress to point P at the present time step n. The algorithm is an iterative approximation technique and is described as following:

(i) The position and corresponding variables of point R are calculated in the same way as Equations (9) and (10) with the characteristic speed c.

(ii) Equation (13) is used to approximate the water depth at point P.

$$h_P = h_R - h_R\left(\frac{u_M^{n-1} - u_{M-1}^{n-1}}{\Delta x}\right)\Delta t \tag{14}$$

(iii) The position and corresponding variables of point L are calculated in the same way as Equations (9) and (10) with the characteristic speed c^+.

(iv) With the result of Step (ii), Equation (12) is used to approximate the discharge at point P.

$$q_P = q_L - a^+(h_P - h_L) + f \tag{15}$$

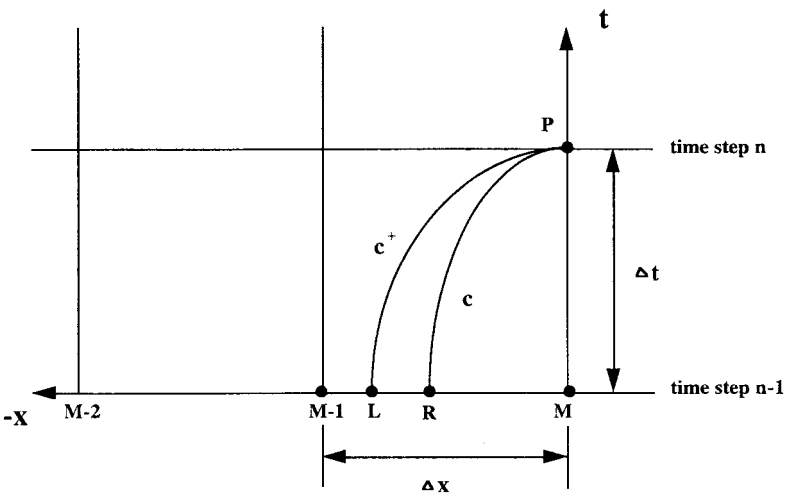

Figure 2. Sketch of characteristic curves near the downstream boundary.

where

$$f = gh(S_o - S_f)\Delta t$$

The values of c, c^+, a^+ and f are calculated by variables at point M for the first approximation, and should be adjusted in the proceeding iterations to obtain the correct flow conditions. Hence the following steps:

(v) The values of c^+, a^+ and f are recalculated by averaging those at points L and P with the last approximated dependent variables.

$$c^+ = \frac{1}{2}[(u + \sqrt{gh})_L + (u + \sqrt{gh})_P]$$

$$a^+ = \frac{1}{2}[(-u + \sqrt{gh})_L + (-u + \sqrt{gh})_P]$$

$$f = \frac{1}{2}g\{[h(S_o - S_f)]_L + [h(S_o - S_f)]_P\}$$

(vi) Repeat Steps (iii) to (v) until discharge at point P converges.
(vii) The value of c is recalculated by averaging the last approximated dependent variables at points R and P.
(viii) Repeat Steps (i) to (vii) until the water depth at point P converges.

3.3. *Algorithm*

Given the proper initial conditions, the solution procedure of the proposed iterative explicit scheme involves the following steps:

(i) Determine the flow conditions at the boundaries.

(ii) Estimate $q_{\xi 1}$ using Equations (9) and (10).
(iii) Compute $q_2^{n'}, q_3^{n'}, \ldots$, from Equation (8).
(iv) Compute $h_{3/2}^{n'}, h_{5/2}^{n'}, \ldots$, from Equation (7), using the updated $q_i^{n'} (i = 2, 3, \ldots)$ from Step (iii).
(v) Repeat Steps (ii) to (iv) until the following criterion is satisfied:

$$\frac{|(q_i^{n'})_{\text{new}} - (q_i^{n'})_{\text{old}}|}{(q_i^{n'})_{\text{old}}} \leqslant \varepsilon, \quad \text{for } i = 2, 3, \ldots \tag{16}$$

$$\frac{|(h_{i+1/2}^{n'})_{\text{new}} - (h_{i+1/2}^{n'})_{\text{old}}|}{(h_{i+1/2}^{n'})_{\text{old}}} \leqslant \varepsilon, \quad \text{for } i = 1, 2, \ldots \tag{17}$$

where the subscripts 'new' and 'old' denote the present and the previous iterations, respectively; and ε is the allowable error, which was set to 10^{-6} in this study.
(vi) Let $q_{i+1}^n = (q_{i+1}^{n'})_{\text{new}}$, $h_{i+1/2}^n = (h_{i+1/2}^{n'})_{\text{new}}$, and $u_{i+1}^n = (u_{i+1}^{n'})_{\text{new}}$, for $i = 1, 2, \ldots$
(vii) Repeat Steps (i) to (vi) for the next time Step $(n + 1)$.

3.4. Stability analysis

From Equations (9) and (10), it can be seen that the foot of the characteristics line, $x_{\xi 1}$, must lie between x_i and x_{i-1} to ensure the stability of the convection-dominated momentum equation as shown in Equation (8). Therefore $|u|\Delta t/\Delta x \leqslant 1$ is a necessary condition for the stability of Equation (8), which can be proved by the Fourier analysis with the Von Neumann condition (see Appendix A).

Similar to other explicit numerical method applied to the open-channel flow, the Courant condition, defined as $Cr = (|u| + \sqrt{gh})\Delta t/\Delta x \leqslant 1$ by the larger absolute value of the characteristic speeds, $u \pm \sqrt{gh}$, is the limit on determining the time step. When the Courant condition is satisfied, the stability condition, $|u|\Delta t/\Delta x \leqslant 1$, for the proposed scheme will be satisfied, too. Hence the proposed scheme is proved to be valuable under the Courant condition.

4. ANALYTICAL SOLUTIONS

To examine the accuracy of the proposed scheme, the analytical solutions of surges and dam-break flows in horizontal, rectangular, and frictionless channels are used. The exact solution of surge celerity (u_s) and surge height (h_1) can be obtained by simultaneously solving the following two equations based on the conservation of mass and momentum:

$$u_s = \frac{q_2 - q_1}{h_2 - h_1} \tag{18}$$

$$u_s = \frac{\left(\dfrac{q_2^2}{h_2} + \dfrac{1}{2} g h_2^2\right) - \left(\dfrac{q_1^2}{h_1} + \dfrac{1}{2} g h_1^2\right)}{q_2 - q_1} \tag{19}$$

where the subscripts 1 and 2 represent the upstream and downstream sides of the surge, respectively. For the dam-break problem, one needs an additional equation describing the movement of the negative simple wave:

$$u - 2c = u_0 - 2c_0 = \text{const.} \tag{20}$$

where u_0 and c_0 are the initial velocity and the surface-disturbance wave celerity in the reservoir, respectively; and $c = \sqrt{gh}$. Thus, the water surface profile of the negative simple wave can be determined by

$$\frac{\mathrm{d}x}{\mathrm{d}t} = u + c = 3c + u_0 - 2c_0 \tag{21}$$

5. EXAMPLES AND SIMULATION RESULTS

The advantage of the proposed iterative explicit scheme is its simplicity in formulation and fast convergence in numerical iterations. Nevertheless, two parameters, i.e., the Courant number Cr and weighting factor θ in Equations (7) and (8), in the proposed scheme need to be examined for further applications. Suggestion of the two values is possible by comparing the relative accuracy of the simulated results for cases to analytic solutions. To simplify the analysis and to compare the numerical solutions with the exact solutions of surges and dam-break flows, bed slope and resistance are neglected first. The proposed scheme performs well in the simulations of (1) downstream surge propagation due to the sudden opening of a gate, (2) upstream surge propagation due to the sudden closure of a gate, and (3) dam-break flow in a wet or even dry downstream channel bed, when compared with the analytic solutions and numerical solutions obtained by other schemes. Furthermore, to account for more realistic flow situation and to compare with the experimental data of dam-break flow waves, bed slope and resistance effects are taken into account.

5.1. Flows in a horizontal and frictionless channel

5.1.1. Sudden opening of a gate. The sudden opening of a gate to convey water into a channel from still waters at a constant depth results in the formation of a surge that propagates downstream. Further opening of the gate will convey even more water and, consequently, create a higher surge that will pass over the previous surge. Figure 3 sketches a gate or a dam located somewhere in a channel. The example assumes that the gate is initially closed with a still tailwater of 1 m in depth (h_2) and a surge of $q_1 = 20\,\mathrm{m^2\,s^{-1}}$. According to Equations (18) and (19), one can find that $u_s = 8.48\,\mathrm{m\,s^{-1}}$ and $h_1 = 3.36\,\mathrm{m}$. The traveling distance of the surge front can be determined by multiplying u_s by the elapsed time after the sudden opening of the gate. Note that the surge propagation in this example is in the supercritical-flow regime and is more difficult to solve from the viewpoint of numerical stability and accuracy.

Numerical testing of various Cr's and θ's based on the above example shows that $Cr = 0.5$ and $\theta = 0.9$ yield the best accuracy in comparison with the analytic solution. Therefore, these two calibrated values are recommended for use in future analyzes on surge problems. Figure 4 demonstrates the simulated results for $\theta = 0.5, 0.7$, and 0.9 given $Cr = 0.5$ after 10 seconds of gate opening; it can be seen that the phase error of the surge front slightly decreases

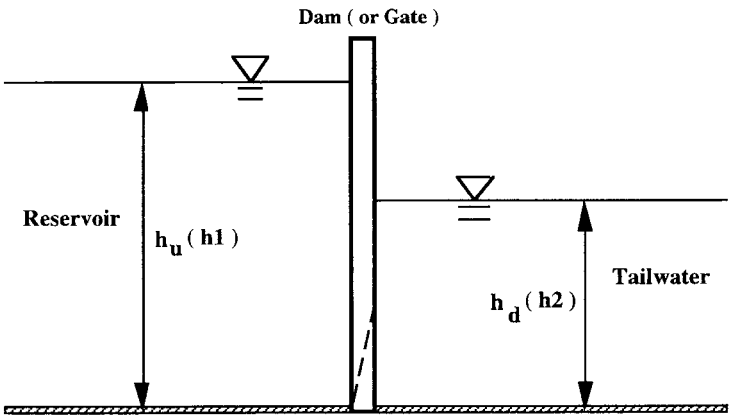

Figure 3. Sketch of surge or dam-break problem.

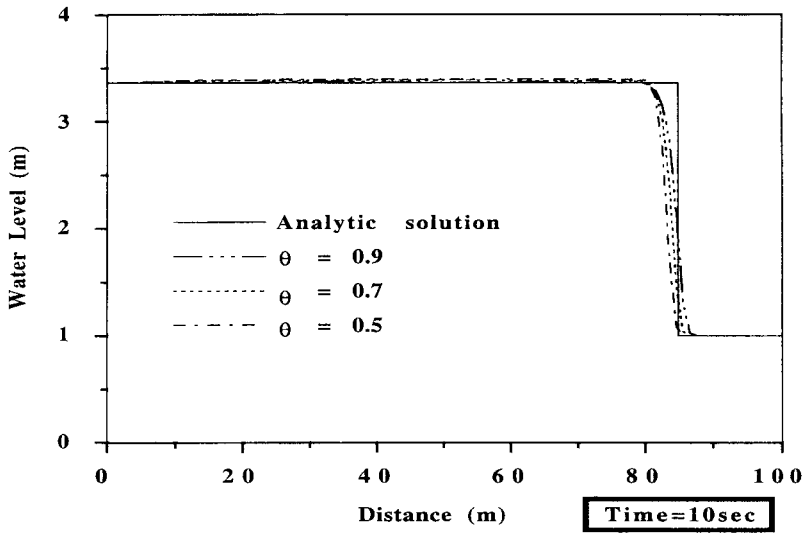

Figure 4. Simulated results of surge propagation for $Cr = 0.5$.

as θ increases. On the other hand, Figure 5, as an illustration, shows the simulated results for $Cr = 0.4, 0.5$, and 0.6 given $\theta = 0.9$ at the same time as in Figure 4; the simulated surge celerity is a little slower for the case of $Cr = 0.4$, and is a little faster for the case of $Cr = 0.6$.

One of the other tested cases was used to demonstrate the validation of using $Cr = 0.5$ and $\theta = 0.9$. Reducing q_1 from $20\,\mathrm{m^2\,s^{-1}}$ to $2\,\mathrm{m^2\,s^{-1}}$ and keeping other conditions unchanged as in the above example, exact values of u_s and h_1 was determined to be $4.23\,\mathrm{m\,s^{-1}}$ and 1.47 m, respectively. Figure 6 shows the simulated results of the proposed scheme and the Preissmann scheme after 10 seconds of gate opening. The Preissmann scheme used a time-weighting factor

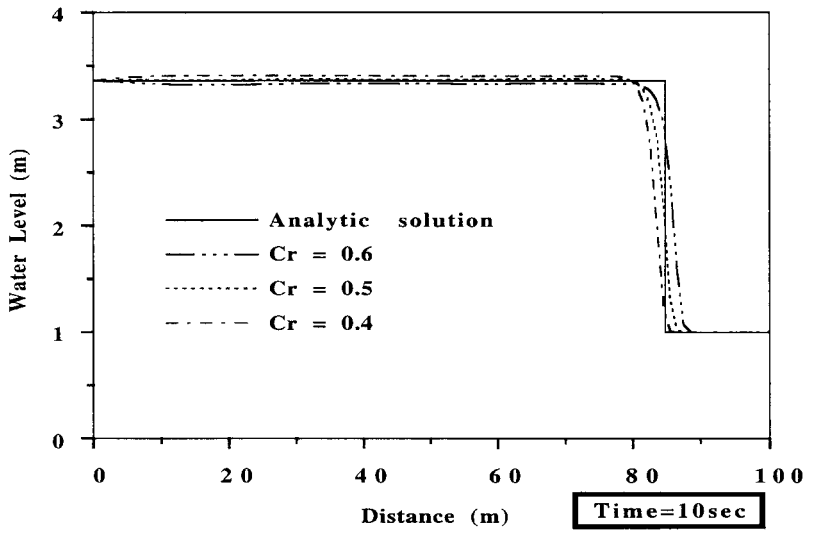

Figure 5. Simulated results of surge propagation for $\theta = 0.9$.

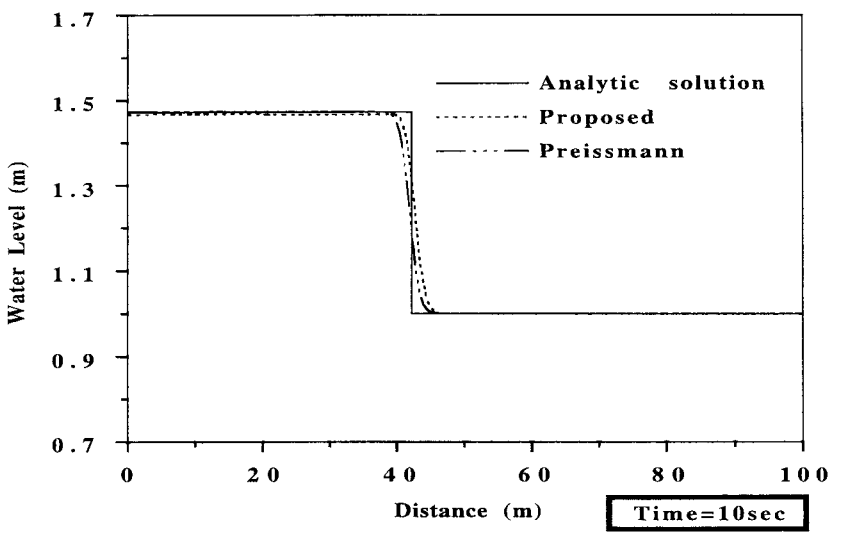

Figure 6. Comparison of simulated results for downstream propagating surge.

of 0.7 to avoid the numerical oscillations near the surge front. Time increment $\Delta t = 0.2$ s was used in the Preissmann scheme. Even though the Preissmann scheme is slightly more accurate than the proposed scheme in the surge celerity, the simulated result by the proposed scheme is still satisfactory compared with the analytic solution.

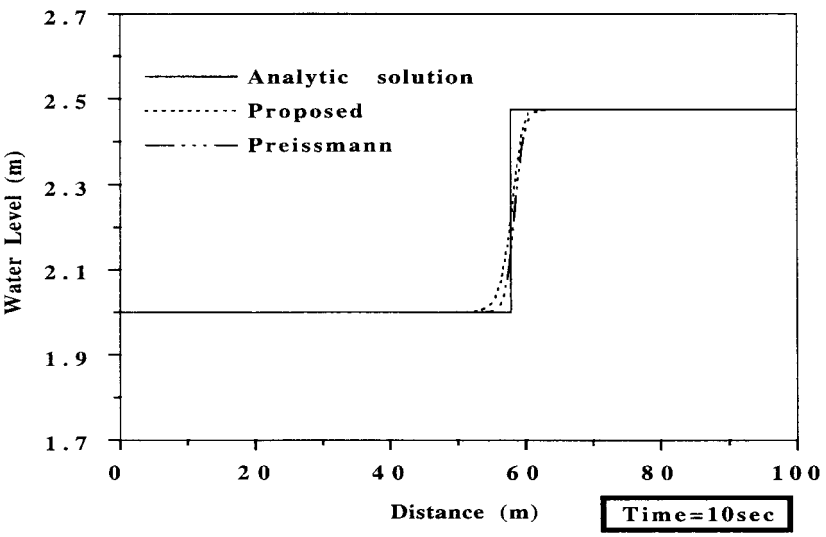

Figure 7. Comparison of simulated results for upstream propagating surge.

5.1.2. Sudden closure of a gate. A uniform flow is assumed to have $q_1 = 2\,\mathrm{m^2\,s^{-1}}$ and $h_1 = 2\,\mathrm{m}$ in a channel. The sudden closure of a gate may occur at the downstream end of the channel due to some unexpected reasons, e.g., an abrupt shutdown of a hydro-power plant connected to the channel. Such an emergent operation of the gate will result in a upstream propagating surge. The exact value u_s and h_2 is $4.23\,\mathrm{m\,s^{-1}}$ and 2.47 m, respectively. The calibrated values of $Cr = 0.5$ and $\theta = 0.9$ for surge problems are used for the proposed scheme. On the other hand, the time increment Δt and the time-weighting factor for the Preissmann scheme is 0.15 s and 0.7, respectively. The space increment Δx is 1 m for both schemes. Figure 7 shows the simulated results by the proposed scheme and the Preissmann scheme after 10 seconds of gate closure. It can be seen that the proposed scheme performs slightly better than the Preissmann scheme with less phase error of the surge front. In this example, the satisfactory simulated result validates the above calibrated parameters.

5.1.3. Dam-break flow on wet bed. Computation of dam-break flood waves resulting from the sudden collapse of a dam is necessary for the dam-safety evaluation. The ratio of h_d/h_u (Figure 3) is an important index to judge the applicability and accuracy of the numerical schemes to the dam-break problem. As mentioned earlier, both subcritical- and supercritical-flow regimes exist simultaneously in a rectangular, horizontal, and frictionless channel when h_d/h_u is smaller than 0.138 [32]. In such a mixed flow regime, some of the existing schemes will encounter the numerical stability problem. In particular, as can be seen later, the simulation accuracy will usually decrease significantly as h_d/h_u approaches zero for most of the existing numerical schemes.

To compare the simulated results of the proposed scheme with that of other schemes, the example in Jha *et al.* [11] will be used. In addition to Jha *et al.*'s flux splitting scheme for comparison, the results obtained by the MacCormack and the Gabutti schemes mentioned in Jha *et al.* [11] will also be included. In the example, a 2000-m-long channel is assumed to

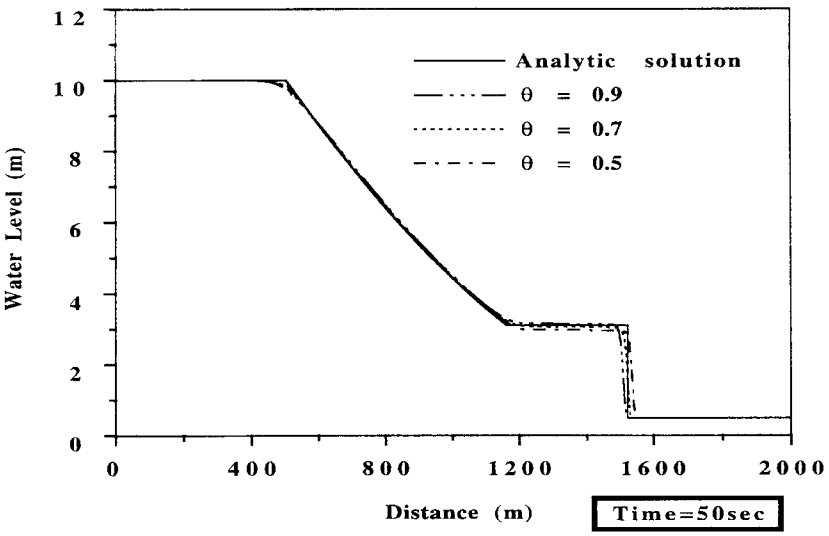

Figure 8. Simulated results of dam-break flow for $Cr = 0.7$.

be separated by a dam located in the middle of the channel, as shown in Figure 3. The initial depth (h_u) in the reservoir is assumed to be 10 m, and the tailwater depth (h_d) is varied with the ratios of $h_d/h_u = 0.5, 0.05$, and 0.005. As was pointed out by Jha *et al.* [11], the MacCormack and the Gabutti schemes failed to execute when h_d/h_u was less than 0.05. If a proper artificial diffusion term was added, both schemes could work, even for smaller ratios of h_d/h_u. However, the Gabutti scheme would still fail when h_d/h_u was equal to or less than 0.005. Jha *et al.*'s flux splitting scheme, on the other hand, has no limitations on h_d/h_u except for the critical case of $h_d = 0$.

Before comparing the performances of various numerical schemes, the proper values of Cr and θ in the proposed scheme for the dam-break flows need to be examined first. The case of $h_d/h_u = 0.05$ was used for calibrating the values of Cr and θ. The distance increment (Δx) used in the simulation was 5 m, and this value was also adopted by the proposed scheme in later analysis. By varying Cr and θ for test cases, one can conclude that the simulated results under $Cr = 0.7$ and $\theta = 0.7$ accurately fit the analytic solution. Hence, these two calibrated values are recommended for use in further analyzes on dam-break problems. Figures 8 and 9 demonstrate that the shape and celerity of the dam-break wave are insensitive to both Cr and θ values. Figure 8 shows the variation of the solutions due to using different θ's with $Cr = 0.7$. One can see that the simulated surge height and celerity are more accurate when $\theta = 0.7$. On the other hand, Figure 9 shows the variations of the solutions due to using different Cr's with $\theta = 0.7$. The best resolution of the simulated surge height and celerity occurs when $Cr = 0.7$.

Figures 10–12 illustrate the comparisons among the simulated results obtained by the proposed scheme and the other schemes, as well as the analytic solutions, for $h_d/h_u = 0.5, 0.05$, and 0.005, respectively. The superiority of the proposed scheme can be realized from these comparisons. As shown in Figure 10(a), when $h_d/h_u = 0.5$, the Gabutti scheme yields the

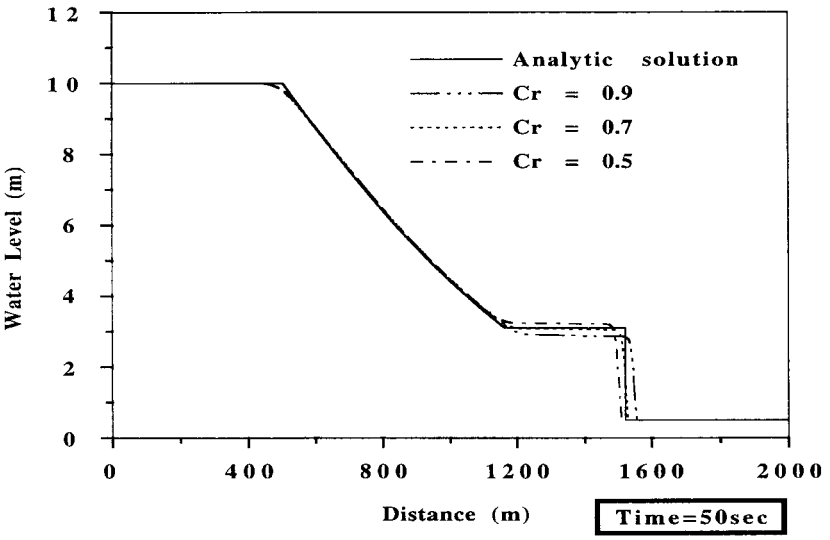

Figure 9. Simulated results of dam-break flow for $\theta = 0.7$.

numerical oscillations at the surge front and the slower celerity of the surge front compared to the exact solution. Figure 10(b) shows the corresponding velocity distribution along the channel when $h_d/h_u = 0.5$. The oscillations of the velocity near the surge front by the Gabutti scheme are clearly observed. When $h_d/h_u = 0.05$, the errors in the location and the height of the surge front obtained by the MacCormack and the Gabutti schemes, as can be seen in Figure 11, are significant. The results obtained by Jha *et al.*'s flux splitting scheme are similar to those obtained by the MacCormack scheme when $h_d/h_u = 0.5$ and 0.05, and thus are not shown in Figures 10 and 11. Figure 12 shows that Jha *et al.*'s scheme performs less satisfactory than the MacCormack scheme when $h_d/h_u = 0.005$. Furthermore, Figure 13 demonstrates the accuracy of the proposed scheme when $h_d/h_u = 0.001$. Instead of using the flux splitting scheme, Jha *et al.* [9] proposed another scheme based on the modifications of the Beam-Warming scheme for the same dam-break example, except that h_u was changed to 15 m. The simulated results were improved, as can be seen in their paper.

5.1.4. Dam-break flow on dry bed. As mentioned earlier, most of the existing numerical schemes fail when the downstream channel of the dam is initially an dry bed, i.e., $h_d = 0$. However, the proposed scheme does not have such a limitation. We used the same dam-break example above, but with the initial condition $h_d = 0$, to demonstrate the capability of the proposed scheme. Figure 14(a) and 14(b) show the simulated water-surface profile and the corresponding velocity profile along the channel, respectively, after 50 s of dam failure. The results obtained by the proposed scheme are still accurate compared with the analytic solution. In order to compare with the results obtained by Zhang *et al.* [34] using an analog of the SIMPLER method, we need to non-dimensionalize the ordinate and abscissa of Figure 14(b) by dividing them by $\sqrt{gh_u}$ and $t\sqrt{gh_u}$, respectively, where t is the time elapsed

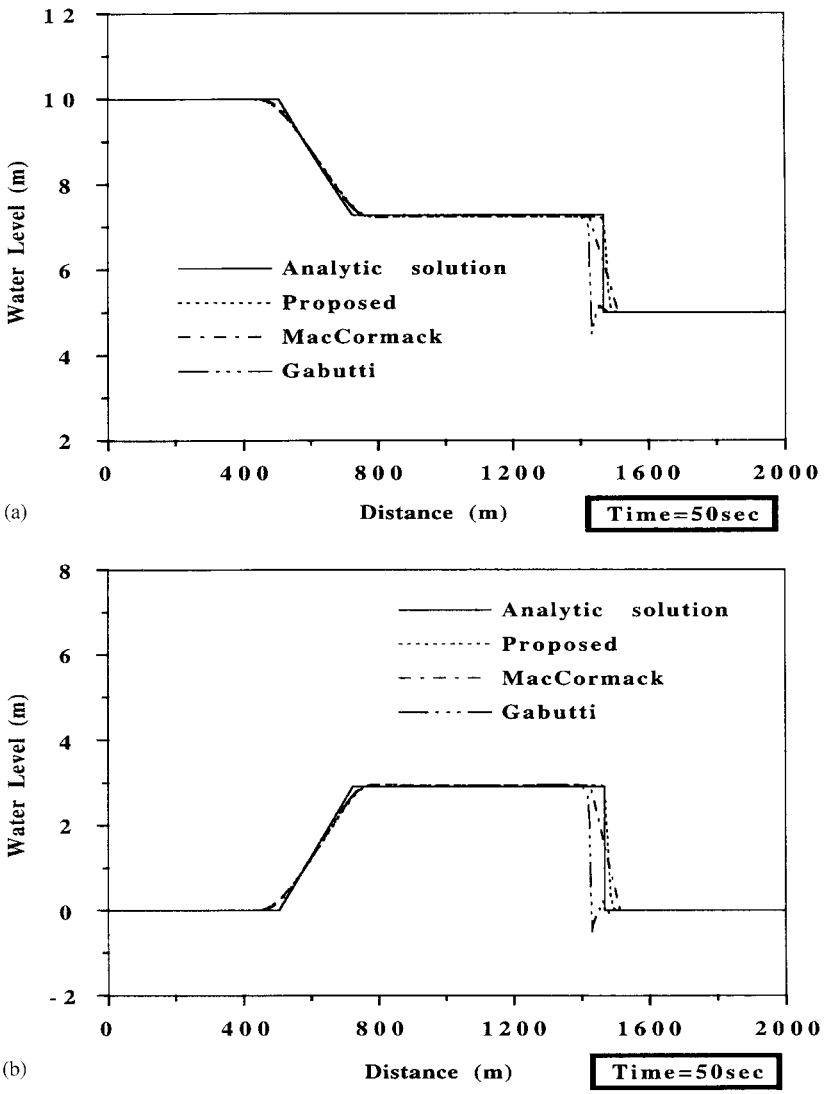

Figure 10. (a) Comparison of simulated water-surface profiles for dam-break flow with $h_d/h_u = 0.5$; (b) comparison of simulated velocity profiles for dam-break flow with $h_d/h_u = 0.5$.

after the sudden dam break. Figure 15 shows the comparison of the simulated results of the two schemes. Again, the excellent performance of the proposed scheme under the dry-bed condition is observed.

5.2. Dam-break flow on dry bed in a sloped and frictional channel

The examples demonstrated in the previous sections verified the proposed scheme under the condition of neglecting the effects of the bed and friction slope in the Saint Venant equation.

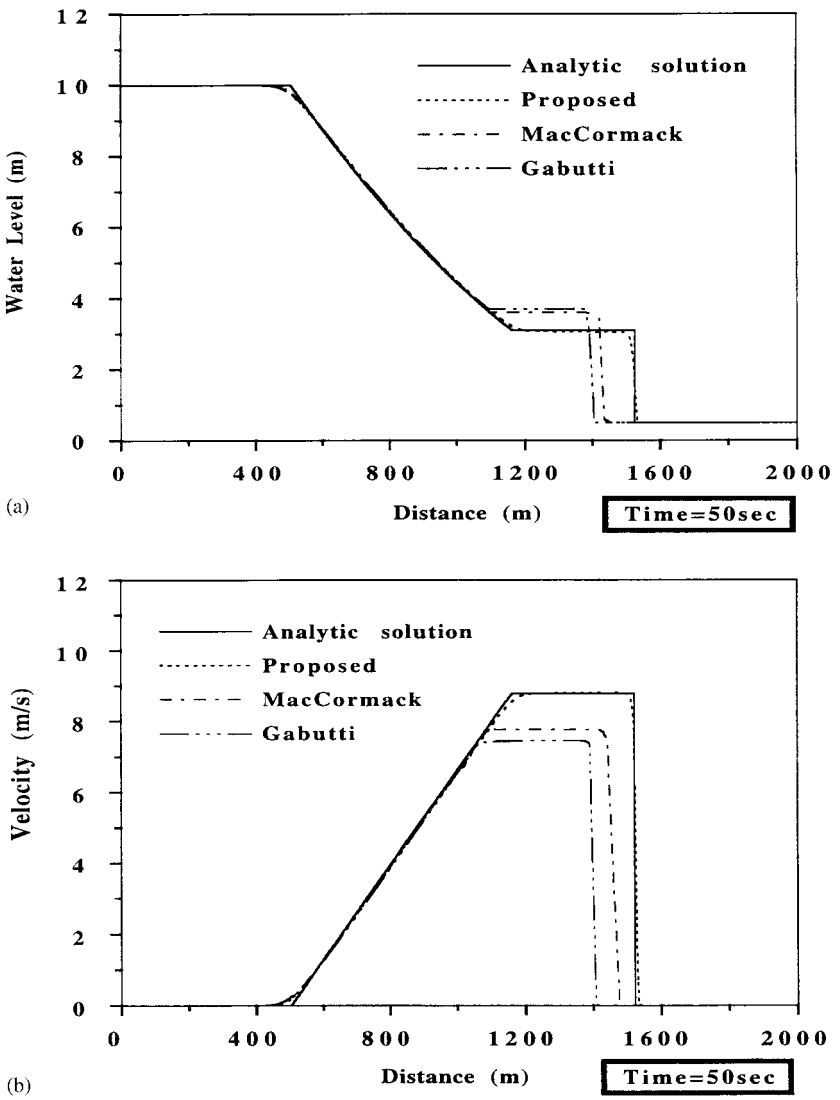

Figure 11. (a) Comparison of simulated water-surface profiles for dam-break flow with $h_d/h_u = 0.05$; (b) comparison of simulated velocity profiles for dam-break flow with $h_d/h_u = 0.05$.

By comparison with the analytic solutions, two important parameters Cr and θ were examined. With the suggested values of them, it has been found that the proposed scheme simulated most the illustrated cases with excellent accuracy, even the critical flow conditions. However, more important, the capability of simulating flow conditions in a sloped and frictional channel makes the extension of the proposed model to practical applications possible and will be investigated in the section.

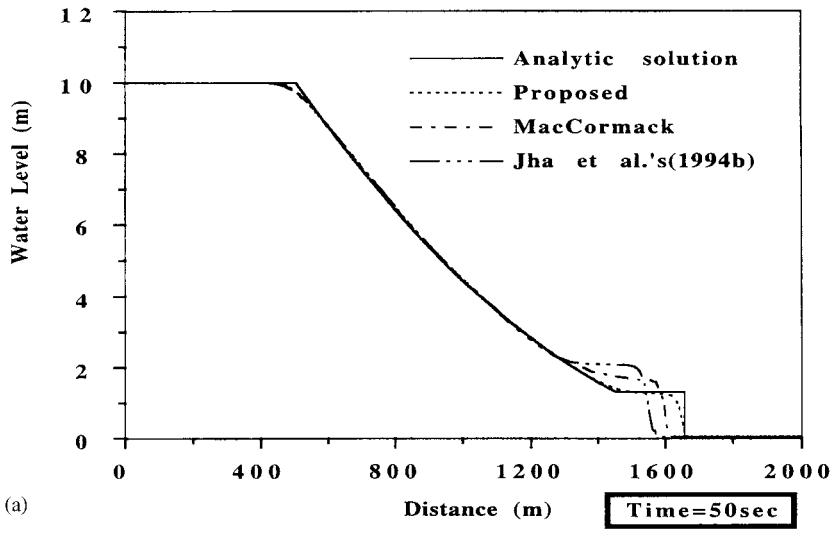

(a)

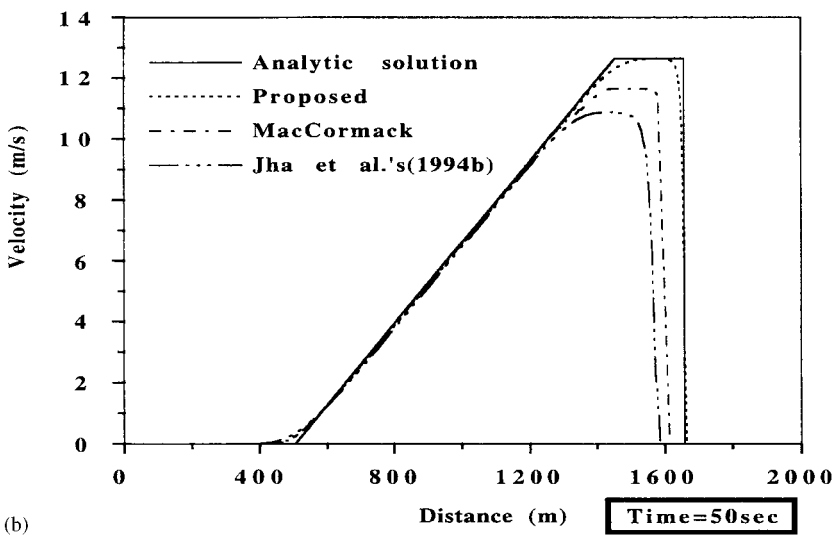

(b)

Figure 12. (a) Comparison of simulated water-surface profiles for dam-break flow with $h_d/h_u = 0.005$; (b) comparison of simulated velocity profiles for dam-break flow with $h_d/h_u = 0.005$.

The laboratory data under WES test condition 1.1 in 1960–1961 [41] are used to verify the simulated results of the proposed scheme, as well as Cheng-lung Chen's scheme [43] developed on the basis of an explicit scheme of the characteristics method. WES conducted dam-break flood-wave experiments in a 400-ft (122-m) long, 4-ft (1.22-m) wide, sloped (0.005), and rectangular flume with a 1-ft (0.305-m) high model dam located midway of its length. The model dam was lifted almost instantaneously by a pulley-weight system to simulate the

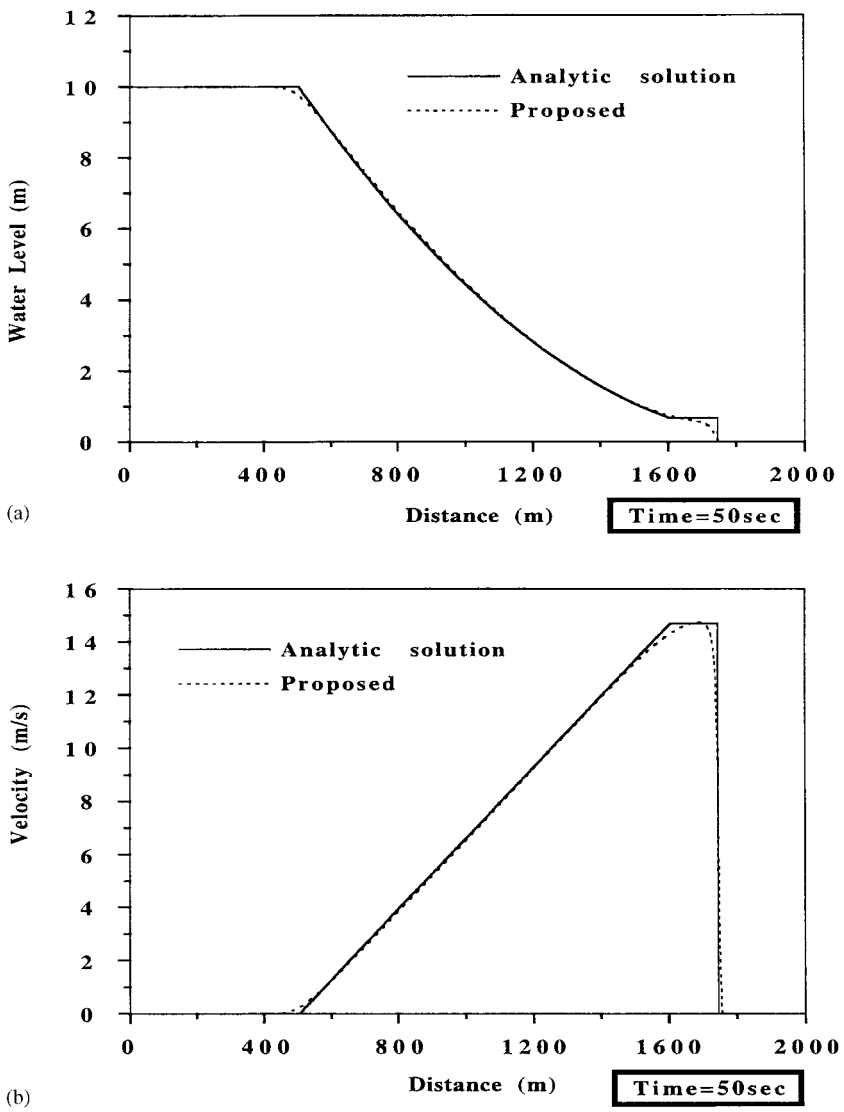

Figure 13. (a) Simulated water-surface profile for dam-break flow with $h_d/h_u = 0.001$; (b) simulated velocity profile for dam-break flow with $h_d/h_u = 0.001$.

sudden dam failure. Under WES test condition 1.1, width of breach is 4-ft (1.22-m), depth of breach is 1-ft (0.305-m), and the channel roughness, Manning coefficient, is 0.009. The values of parameters Cr and θ for the proposed scheme maintained 0.7 that was recommended in the previous section.

Figure 16(a) and 16(b) show the water surface profiles and their corresponding velocity distributions at 0, 10, 20, 30, 50, 90, and 160 s after dam break, respectively. The initial

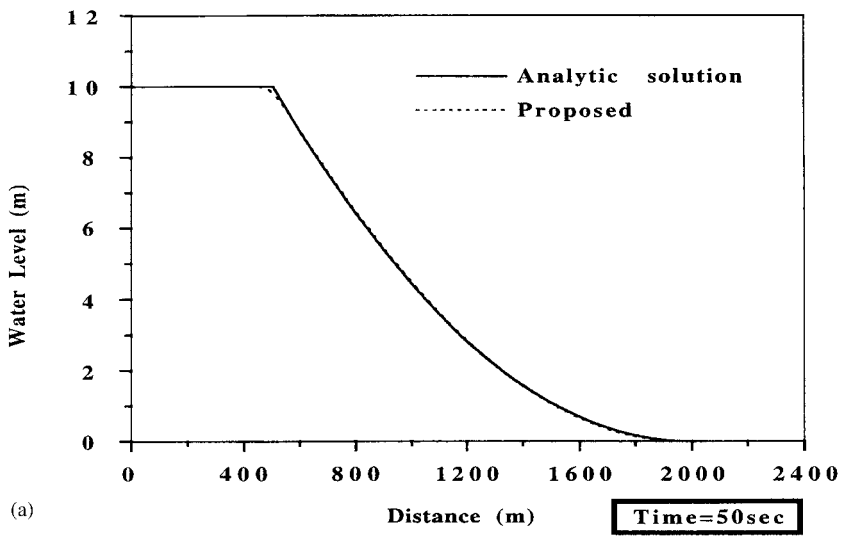

(a)

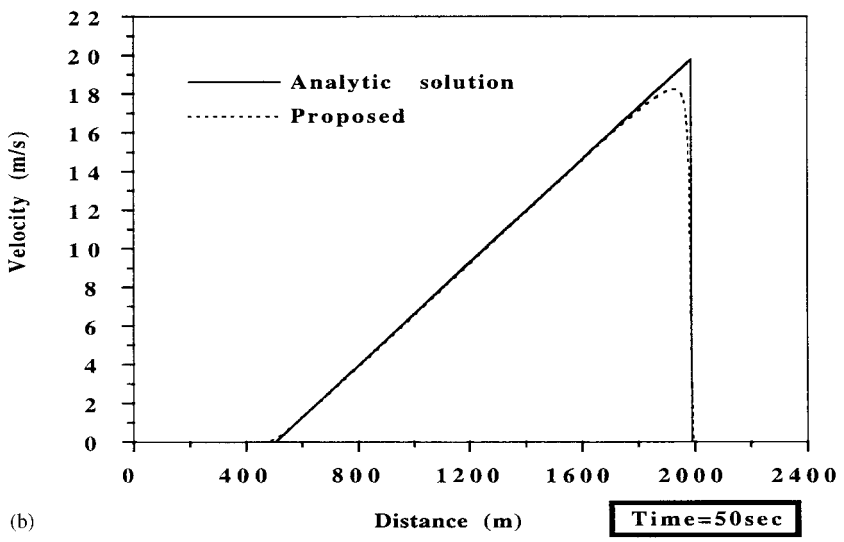

(b)

Figure 14. (a) Simulated water-surface profile for dam-break flow with $h_d = 0$; (b) simulated velocity profile for dam-break flow with $h_d = 0$.

condition in the channel downstream of the dam for the proposed method can be realized from the figures that real dry bed condition, i.e. $u = 0$ and $d = 0$, was given. This is not the case for Chen's scheme, in which a computer-simulated condition Q_o for no initial flow was assumed to be 0.001 cfs. At the trailing edge in the receding part of the flood near the upstream end, the same negligibly small inflow discharge Q_o was also used to circumvent the singularity problem in Chen's scheme. In addition, numerical noise occurs around

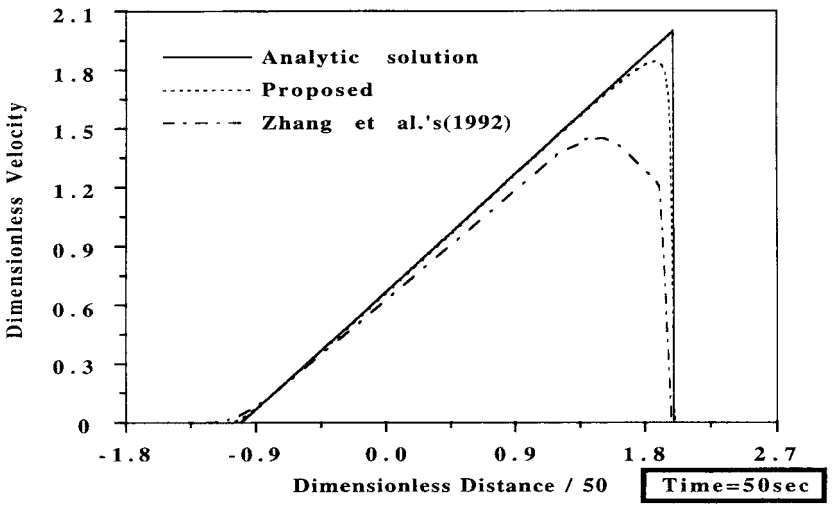

Figure 15. Comparison of dimensionless velocity profiles for dam-break flow with $h_d = 0$.

the front of the wave. The assumptions of small initial flows are not needed in the proposed scheme and numerical noise does not happen either, as can be seen in Figure 16(a) and 16(b).

According to the classification mentioned previously, Chen's cheme is a 'shock fitting' method. The shock equations (often referred to as the Rankine–Hugoniot equations) are adopted to determine the propogation velocity of the shock front, and the conjugate water depths in back and front of the shock. By imposing shock equations, it has been assumed that the flow downstream of the shock front is always uniform under a given flow rate. Therefore, as imposed on a dry bed, shock equations become valid only under some assumptions of flow immediately behind the leading edge. For example, Whitham [42] circumvented this problem by assuming uniform flow velocity in the direction of flow behind the leading edge.

However, the proposed scheme belongs to the 'through' method which solves the Saint Venant equations directly without any particular treatment of the shock front. Figure 17 shows the water depth hydrographs at six stations; three upstream the dam recording the negative wave at $x = 100, 150$ and 200 ft; three downstream the dam recording the positive wave at $x = 225, 280$ and 350 ft. The water depths obtained from the proposed and Chen's schemes are quite accurate at the upstream stations, and are also close at the downstream stations with slightly small peak depth by the proposed scheme. The arrival time of the positive wave by the proposed scheme at the downstream stations are a little closer to those of the measured data. Figures 18 and 19 show the velocity and discharge hydrographs at the downstream stations, respectively. It can be seen that the peak discharges and corresponding velocities by the proposed scheme are slightly larger than those by Chen's scheme. Of course, the arrival time of the positive wave are the same as for depth hydrographs and still a little closer to those of the measured data. In general, the two numerical schemes have similar performance and have considerably reasonable results compared with the measured data.

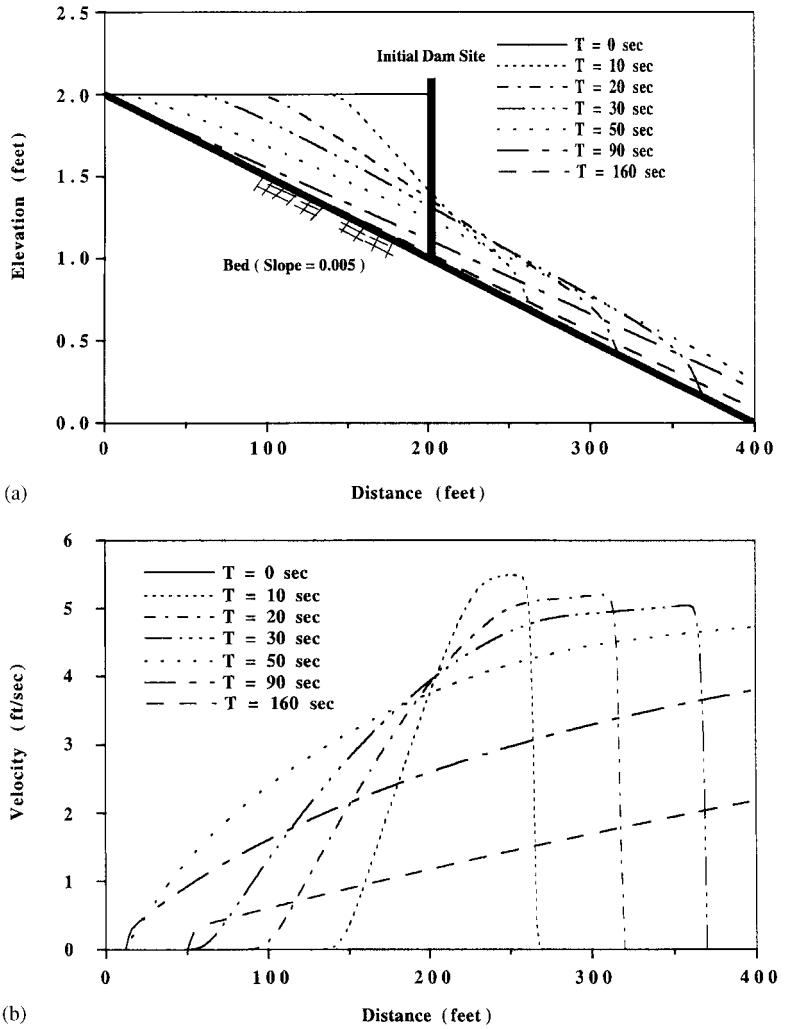

Figure 16. (a) Water-surface profiles at different time for flood under WES test condition 1.1; (b) velocity distributions at different time for flood under WES test condition 1.1.

6. CONCLUSIONS

The objective of this paper is to propose an iterative explicit scheme suitable for solving 1D unsteady open-channel flow problems based on the Saint Venant equations, especially for the surges and dam-break flows. For each time step, the proposed scheme first solves the momentum equation for discharge per unit width and then the continuity equation for water depth, and the procedure is iterated until convergence is reached. A staggered-grid system was adopted in the scheme to avoid the 'checkerboard' phenomenon.

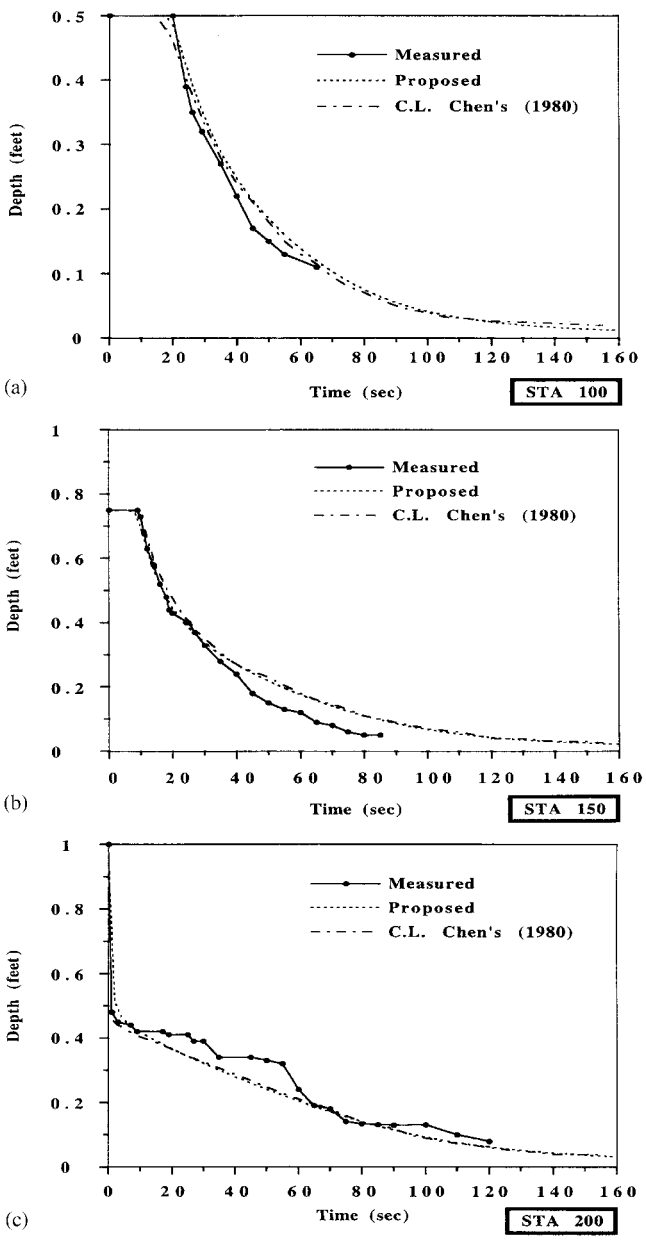

Figure 17. (a) Stage hydrographs at station $x = 100$ ft for flood under WES test condition 1.1; (b) stage hydrographs at station $x = 150$ ft for flood under WES test condition 1.1; (c) stage hydrographs at station $x = 200$ ft for flood under WES test condition 1.1; (d) stage hydrographs at station $x = 225$ ft for flood under WES test condition 1.1; (e) stage hydrographs at station $x = 280$ ft for flood under WES test condition 1.1; (f) stage hydrographs at station $x = 350$ ft for flood under WES test condition 1.1.

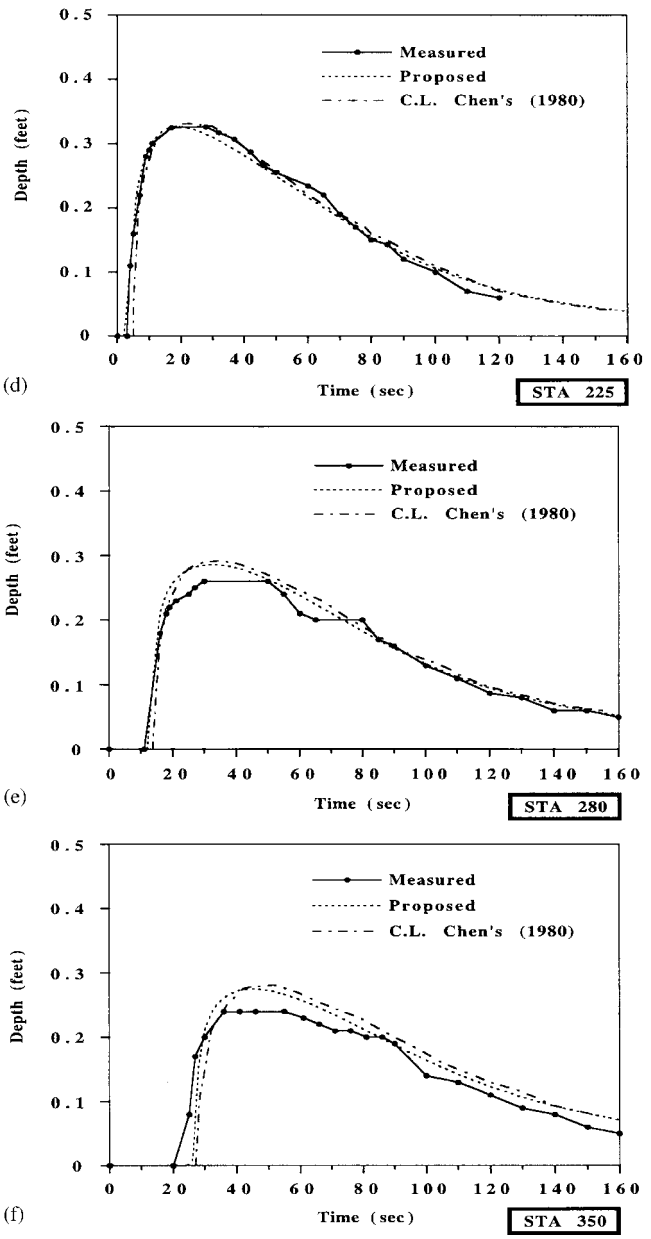

Figure 17. (*Continued*).

To determine the parameters Cr and θ, comparisons were made between the proposed scheme and other schemes against the analytic solution for surge and dam-break flows in the horizontal, rectangular, and frictionless channel. For the surge problem, the suggested values

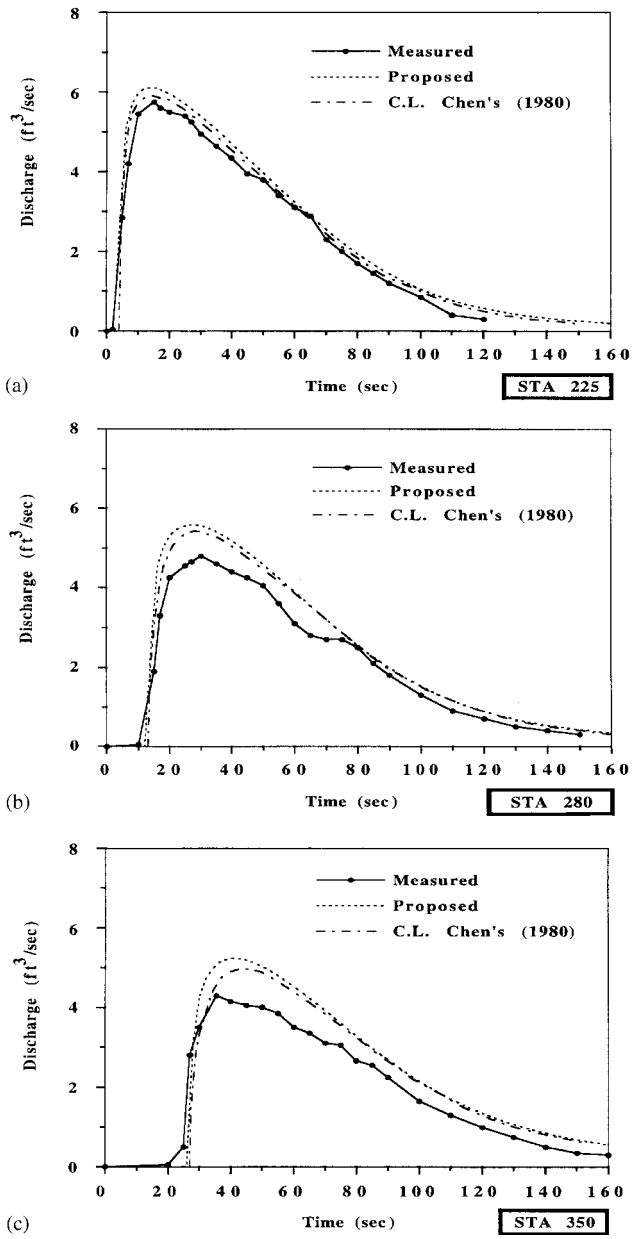

Figure 18. Discharge hydrographs at stations (a) $x = 225$ ft, (b) $x = 280$ ft, (c) $x = 350$ ft downstream of breach for flood under WES test condition 1.1.

for Cr and θ in the proposed scheme were 0.5 and 0.9, respectively. For the dam-break problem, the suggested Cr and θ were both 0.7. Three ratios of h_d/h_u, i.e., 0.5, 0.05, and 0.005, were used. As h_d/h_u approached zero, the error associated with the predicted front

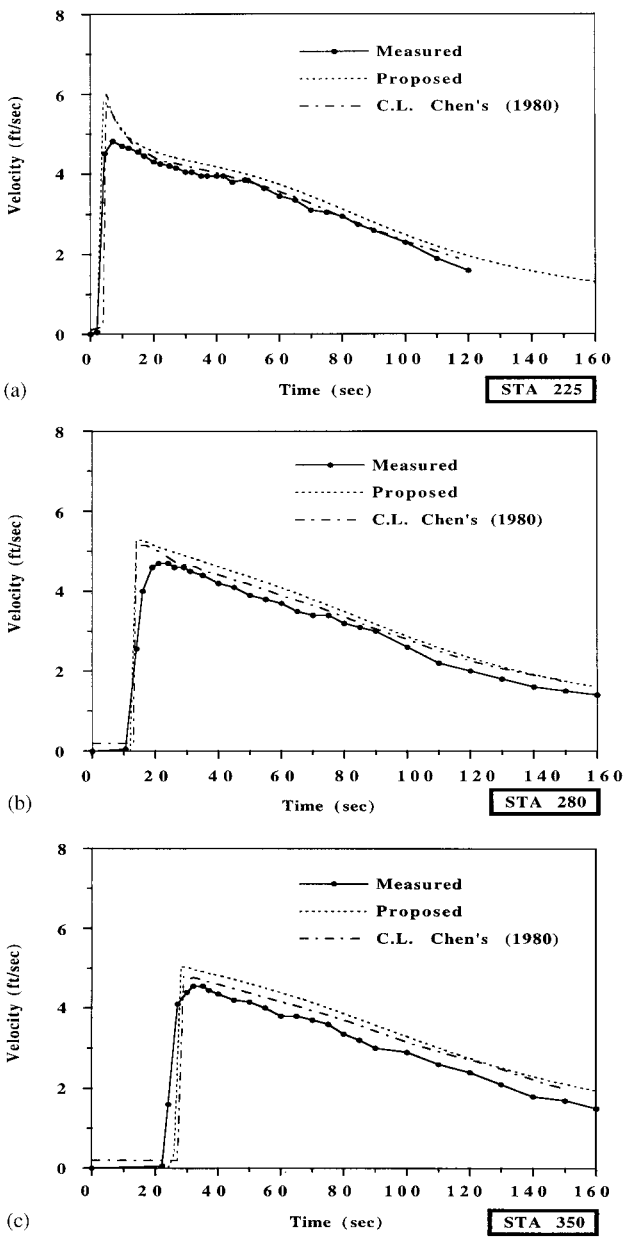

Figure 19. Velocity hydrographs at stations (a) $x = 225$ ft, (b) $x = 280$ ft, (c) $x = 350$ ft downstream of breach for flood under WES test condition 1.1.

height and celerity increased, except by the proposed scheme. In particular, when compared with the results obtained by Zhang *et al.*'s [34] modified SIMPLER scheme under the dry bed condition, the proposed scheme still has satisfactory accuracy.

Further investigations of the capability of the proposed scheme to more realistic channels with bed slope and frictional effects were carried out to demonstrate the extension of this scheme to other potential practical applications are possible. The laboratory data, WES test condition 1.1 in 1960–1961 recording the flow conditions of the dam-break flood waves on a dry bed, were used to verify the numerical schemes. Performance of the proposed scheme is satisfactory compared with the measured data. Because of its algorithmic simplicity and its accuracy for modeling surge and dam-break problems, the proposed scheme may serve as an attractive alternative to other practical, unsteady open-channel problems.

APPENDIX A

The iterative, explicit, characteristics-based finite-difference scheme, Equation (8), for the Saint Venant dynamic equation is stable if $[(|u|\Delta t)/(\Delta x)] \leqslant 1$.

[Proof] Equation (8) is rewritten in the expression with the discharge q being the unknown variable only.

$$q_j^{n'} = q_{\xi 1} + [\theta q_j^{n'} + (1-\theta) q_{\xi 1}] C_1 \cdot \Delta t + [\theta q_j^{n'2} + (1-\theta) q_{\xi 1}^2] C_2 \cdot \Delta t + S \cdot \Delta t \tag{A1}$$

where C_1 and C_2 are regarded as constants, and S is the hydrostatic pressure term and is neglected hereinafter in the proof. The Fourier transform taking r as the so-called amplification factor is defined as

$$q_j^n = \Sigma r^n(\beta) e^{ij\Delta x\beta} \tag{A2}$$

where β is the wave number, and r may be complex. Consider u being positive and $v = u\Delta t/\Delta x \leqslant 1$, the following inequality is obtained.

$$0 \leqslant 1 - 4v(1-v)\sin^2 \frac{\Delta x\beta}{2} \leqslant 1 \tag{A3}$$

Taking the Fourier transforms of Equation (A1) without the term $S\Delta t$ yields

$$\begin{aligned} r &= (1-v) + ve^{-i\Delta x\beta} + \{\theta r' + (1-\theta)[(1-v) + ve^{-i\Delta x\beta}]\} C_1 \cdot \Delta t \\ &\quad + \{\theta r'^2 e^{i\Delta x\beta} + (1-\theta)[(1-v)e^{i\Delta x\beta} + v]^2 \cdot e^{-i\Delta x\beta}\}\ C_2 \cdot \Delta t \\ &= (1-v) + ve^{-i\Delta x\beta} + \{\theta r' + (1-\theta)[(1-v) + ve^{-i\Delta x\beta}]\}\ C_1 \cdot \Delta t \\ &\quad + \{\theta r'^2 e^{i\Delta x\beta} + (1-\theta)(1-v) \cdot [(1-v)e^{i\Delta x\beta} + v] \\ &\quad + (1-\theta)v \cdot [(1-v) + ve^{-i\Delta x\beta}]\}\ C_2 \cdot \Delta t \end{aligned}$$

where r' is the amplification factor between the discharge newly updated during iterations and that of the previous time step, and equals one for the first iteration. With the following

relations

$$|v+(1-v)e^{i\Delta x\beta}| = |(1-v)+ve^{-i\Delta x\beta}| = \left[1-4v(1-v)\sin^2\frac{\Delta x\beta}{2}\right]^{1/2}$$

the magnitude of the amplification factor is

$$\begin{aligned}
|r| &\leqslant \left[1-4v(1-v)\sin^2\frac{\Delta x\beta}{2}\right]^{1/2} \\
&\quad + \left\{\theta|r'| + (1-\theta)\left[1-4v(1-v)\sin^2\frac{\Delta x\beta}{2}\right]^{1/2}\right\} C_1\cdot\Delta t \\
&\quad + \left\{\theta|r'|^2 + (1-\theta)(1-v)\cdot\left[1-4v(1-v)\sin^2\frac{\Delta x\beta}{2}\right]^{1/2}\right. \\
&\quad \left. + (1-\theta)v\cdot\left[1-4v(1-v)\sin^2\frac{\Delta x\beta}{2}\right]^{1/2}\right\} C_2\cdot\Delta t \\
&\leqslant 1 + C_1\cdot\Delta t + C_2\cdot\Delta t \\
&= 1 + O(\Delta t)
\end{aligned}$$

By the Von Neumann condition, the scheme is stable. The other case of negative u can be proved to be stable likewise.

ACKNOWLEDGEMENTS

This research is supported by the National Science Council of the Republic of China, under grant No. NSC84-2211-E-009-034. The writers are grateful to W. F. Tsai and C. Y. Shen for their valuable advice during the course of this study.

REFERENCES

1. Cunge JA, Holly FM, Verway A. *Practical Aspects of Computational River Hydraulics.* Pitman: London, 1980.
2. Cunge JA. *Rapidly Varied Flow in Power and Pumping Canals in Unsteady Flow in Open Channel.* Water Resources Publications: Fort Collins, CO, 1975: Ch. 14.
3. Yang JC, Chen KN, Lee HY. An accurate computation for rapidly varied flow in an open channel. *International Journal for Numerical Methods in Fluids* 1992; **14**:361–374.
4. Aguirre-Pe J, Quisca S, Plachco FP. Tests and numerical one-dimensional modelling of a high-viscosity fluid dam-break wave. *Journal of Hydraulics Research* 1995; **33**(1):17–26.
5. Garcia-Navarro P, Saviron JM. McCormack's method for the numerical simulation of one-dimensional discontinuous unsteady open channel flow. *Journal of Hydraulics Research* 1992; **30**(1):95–105.
6. Garcia R, Kahawita RA. Numerical solution of the St. Venant equations with the MacCormack finite-difference scheme. *International Journal for Numerical Methods in Fluids* 1986; **6**:259–274.
7. Fennema RJ, Chaudhry MH. Explicit numerical schemes for unsteady free-surface flows with shocks. *Water Resources Research* 1986; **22**(13):1923–1930.
8. Jha AK, Akiyama J, Ura M. A fully conservative Beam and Warming scheme for transient open channel flows. *Journal of Hydraulics Research* 1996; **34**(5):605–621.
9. Jha AK, Akiyama J, Ura M. Modeling unsteady open-channel flows—modification to Beam and Warming scheme. *Journal of Hydraulics Engineering, ASCE* 1994; **120**(4):461–476.

10. Fennema RJ, Chaudhry MH. Simulation of one-dimensional dam-break flows. *Journal of Hydraulics Research* 1987; **25**(1):41–51.
11. Jha AK, Akiyama J, Ura M. An implicit model based on conservative flux splitting technique for one dimensional unsteady flow. *Journal of Hydroscience Hydraulics Engineering*, *JSCE* 1994; **11**(2):69–82.
12. Alcrudo F, Garcia-Vavarro P, Saviron JM. Flux difference splitting 1D open channel flow equations. *International Journal for Numerical Methods in Fluids* 1992; **14**:1009–1018.
13. Glaister P. Approximate Riemann solutions of the shallow water equations. *Journal of Hydraulics Research* 1988; **26**(3):293–306.
14. Glaister P. Flux difference splitting for open-channel flows. *International Journal for Numerical Methods in Fluids* 1993; **16**:629–654.
15. Mingham CG, Causon DM. A fully conservative Beam and Warming scheme for transient open channel flows. *Journal of Hydraulics Engineering*, *ASCE* 1998; **124**(6):605–614.
16. Mingham CG, Causon DM. Calculation of unsteady bore diffraction using a high resolution finite volume method. *Journal of Hydraulics Research* 2000; **38**(1):49–56.
17. Toro EF. Riemann problems and the WAF method for solving the two-dimensional shallow water equations. *Philosophical Transactions of the Royal Society of London*, *A* 1992; **338**:43–68.
18. Yang JY, Hsu CA, Chang SH. Computations of free surface flows, part 1: one-dimensional dam-break flow. *Journal of Hydraulics Research* 1993; **31**(1):19–34.
19. Hu K, Mingham CG, Causon, DM. A bore-capturing finite volume method for open-channel flows. *International Journal for Numerical Methods in Fluids* 1998; **28**:1241–1261.
20. Savic L, Holly FM. Dambreak flood waves computed by modified Godunov method. *Journal of Hydraulics Research* 1993; **31**(2):187–204.
21. Baines MJ, Maffio A, Di Filippo A. Unsteady 1D flows with steep waves in plant channels: the use of Roe's upwind TVD difference scheme. *Advances in Water Resources* 1992; **15**:89–94.
22. Louaked M, Hanich L. TVD schemes for the shallow water equations. *Journal of Hydraulics Research* 1998; **36**(3):363–378.
23. Garcia-Navarro P, Priestley A, Alcrudo F. An implicit method for water flow modelling in channels and pipes. *Journal of Hydraulics Research* 1994; **32**(5):721–742.
24. Garcia-Navarro P, Priestley A. A conservative and shape-preserving semi-Lagrangian method for the solution of the shallow water equations. *International Journal for Numerical Methods in Fluids* 1994; **18**:273–294.
25. Moin SMA, Lam DCL, Smith AA. Eularian–Lagrangian linked algorithm for simulating discontinuous open channel flows. *Proceedings of the VII International Conference on Computer Methods in Water Resources*, MIT, USA, 1988; **2**:363–368.
26. Hicks FE, Steffler PM. Characteristic dissipative Galerkin scheme for open-channel flow. *Journal of Hydraulics Engineering*, *ASCE* 1992; **118**(2):337–352.
27. Hicks FE, Steffler PM, Yasmin N. One-dimensional dam-break solutions for variable width channels. *Journal of Hydraulics Engineering*, *ASCE* 1997; **123**(5):464–468.
28. Katopodes ND. A dissipative Galerkin scheme for open-channel flow. *Journal of Hydraulics Engineering*, *ASCE* 1984; **110**(4):450–466.
29. Berger RC, Stockstill RL. Finite-element model for high-velocity channels. *Journal of Hydraulics Engineering*, *ASCE* 1995; **121**(10):710–716.
30. Katopodes ND, Wu CT. Explicit computation of discontinuous channel flow. *Journal of Hydraulics Engineering*, *ASCE* 1986; **112**(6):456–475.
31. Alam MM, Bhuiyan MA. Collocation finite-element simulation of dam-break flows. *Journal of Hydraulics Engineering*, *ASCE* 1995; **121**(2):118–128.
32. Henderson FM. *Open Channel Flow.* Prentice-Hall: New Jersey, 1966.
33. Fraccarollo L, Toro EF. Experimental and numerical assessment of the shallow water model for two-dimensional dam-break type. *Journal of Hydraulics Research* 1995; **33**(6):843–864.
34. Zhang H, Youssef H, Long ND, Kahawita R. A 1D numerical model applied to dam-break flows on dry beds. *Journal of Hydraulics Research* 1992; **30**(2):211–224.
35. Patankar SV. *Numerical Heat Transfer and Fluid Flow.* McGraw-Hill Inc.: New York, NY, 1980.
36. Bellos CV, Sakkas FG. 1D dam-break flood wave propagation on dry bed. *Journal of Hydraulics Engineering*, *ASCE* 1987; **113**(12):1510–1523.
37. Di Monaco A, Molinaro P. Finite element solution of the Lagrangian equations of unsteady free-surface flows on dry river beds. *Finite Elements in Water Resources*, K.P. Holz *et al.* (eds). Springer: Berlin, Germany, 1982: 4.25–4.35.
38. Dai W. Numerical Solutions of Unsteady Navier–Stokes Equations Using Explicit Finite Analytic Scheme, PhD Thesis, The University of Iowa, Iowa, 1994.
39. Basco DR. Limitations of de Saint Venant equations in dam-break analysis. *Journal of Hydraulics Engineering*, *ASCE* 1989; **115**(7):950–965.
40. Kobayashi N, Otta AK, Roy I. Wave reflection and run-up on rough slopes. *Journal of Waterway*, *Port*, *Coastal and Ocean Engineering*, *ASCE* 1987; **113**(3):282–298.

41. Floods resulting from suddenly breached dams. Miscellaneous paper No. 2-374. United State Army Corps of Engineers, Waterways Experiment Station, Vicksburg, Miss., Report 1, Conditions of minimum resistance, 1960; Report 2, Conditions of high resistance, 1961.
42. Whitham GB. The effects of hydraulic resistance in dam-break problems. *Proceedings of the Royal Society of London*, *Series A* 1995; **227**:399–407.
43. Chen CL. Laboratory verification of a dam-break flood model. *Journal of Hydraulics Division* 1980; **106**(HY4):535–556.

